

Numerical Analysis of Shallow Foundations in a Soil Mass under Various Behavior Laws

Oustasse Abdoulaye SALL^{1,*}, Déthié SARR², Makhaly BA², Ndiaga CISSE¹, Aboubacry LY¹

¹Department of Civil Engineering, UFR SI, University of Thiès, Thiès, Senegal

²Department of Geotechnical Engineering, UFR SI, University of Thiès, Thiès, Senegal

*Corresponding author: oustaz.sall@univ-thies.sn

Received June 14, 2019; Revised July 18, 2019; Accepted August 13, 2019

Abstract This paper proposes to study the soil-structure interaction (SSI) applied to shallow foundations. To conduct the study, a characterization of the foundation soils is carried out. The finite element study is conducted using the Optum G2 software that allows taking into account the various soil mass behavior. Two types of superficial foundations (individual footing and strip footing) embedded in a homogeneous and stratified soil mass are modeled. The method proceeds to a parametric study of the soil mass by varying the modulus of elasticity, the angle of internal friction, the cohesion, the Poisson's ratio and the failure criteria to study their influences on the mechanical behavior of the foundation. The results obtained show that with the increasing variation of the modulus of elasticity (E), the clay becomes more and more stiff and ductile. For a given stress value, there is a decrease in deformations as the ductility of the clay increases. During the consolidation analysis, it is found that the lower the Young's modulus, more the material is compressible. This shows that the modulus of elasticity of the soil mass depends on its state of consolidation. The study reveals that the constitutive law, the intrinsic properties and the lithology of the soil mass condition the mode of ruin of the structure.

Keywords: shallow foundation, soil-structure interaction, behavior law, modeling, numerical analysis

Cite This Article: Oustasse Abdoulaye SALL, Déthié SARR, Makhaly BA, Ndiaga CISSE, and Aboubacry LY, "Numerical Analysis of Shallow Foundations in a Soil Mass under Various Behavior Laws." *American Journal of Mechanical Engineering*, vol. 7, no. 3 (2019): 129-137. doi: 10.12691/ajme-7-3-3.

1. Introduction

The understanding of the behavior of soils, structures and their interactions therefore plays an increasing and important role in the structural and geotechnical studies of civil engineering works [1]. These interactions between soils and structures are essentially problems of compatibility of deformations, which can only be reliably handled by knowing the deformability of the soils and concrete according to the stress paths followed during construction [1].

The analytical calculation of interfaces (soil-structure interaction) poses many theoretical and mathematical difficulties. Moreover, if this treatment is possible for some ideal configurations, the solutions rarely correspond to the practical requirements. During the last decades, numerical methods have been developed [2-9] to provide approximate solutions to this type of problem. The finite element method is the most used tool in this field. So many software (*Ansys*, *Plaxis*, *Optum G2* ...) have been developed to solve the problems of interfaces (SSI) by the finite element method.

This work is focused on the study of shallow foundations and, more particularly, on the characterization of the soil-structure interface by the finite element method

using Optum G2. An accurate knowledge of the moduli characterizing deformability and stress paths (of the soil and structure) should facilitate the optimization of the structural and geotechnical dimensioning of foundation structures.

The main objective of this work is numerical modeling under Optum G2 of shallow foundations under axial load. It aims more particularly to study the influence of the behavior laws, the geometrical and mechanical characteristics of the foundation and the soil mass on behavior of the whole ground-foundation.

2. Methodology

As part of this work, it is first necessary to characterize the soil in order to elaborate the behavior model of the soil-foundation interface. Contact areas are generally represented by thin-layer interface elements. Constitutive laws as of Mohr-Coulomb, Tresca etc., governs the behavior of the foundation system. The digital resolution of the soil-pile interaction will be made using the Optum G2 software.

2.1. Modeling of Soil Behavior

Generally, the numerical simulation of the behavior of materials is done through rheological models. Sophisticated

models that may represent well the behavior of materials require many parameters that are difficult to determine from a restricted number of tests, and difficult to introduce in a numerical calculation. In what follows, it is presented the main types of behavior laws.

2.1.1. Linear Elastic Model

Elastic materials are materials that return to their original configuration on unloading and obey Hooke's law. Generally, the behavior is said elastic when the history of the loading does not intervene. To a state of stress corresponds only one state of deformation. The elastic behavior can be linear; in this case, the tensor of the deformations is then proportional to the tensor of the stresses during the loading.

The stress - strain relationship is linear, characterized by two parameters:

- an axial modulus of elasticity (Young modulus) E in the case of a compression or simple tensile test, or a shear modulus G for a simple shear test (Figure 1);
- and the Poisson's ratio ν

In reality, this law of behavior does not stick well to reality because even for small deformations, soils have a plastic behavior. In this context, the plastic laws have been proposed to predict the behavior of the soil.

2.1.2. Elastoplastic Model

Tests carried out on solids show that the domain of resilient deformations (or elasticity) is relatively limited. From a certain level of stress, the loading curve is different to the unloading curve.

This type of macroscopic behavior is characteristic of most solids (concretes, soils and rocks, etc.). From a microscopic point of view, the origin of permanent deformations depends on the type of material [5]. For soils, they arise from the modification of the assembly of solid particles. This mode of behavior excludes any effect of aging and viscosity of the material.

2.1.3. Linear Elastic Model, Perfectly Elastic

The perfect linear elastic behavior model was initially developed to describe, in an approximate manner, the

behavior of metals.

However, the existence of a flow stage on the stress - strain behavior curve of many materials has suggested extending this model to concretes, soils and rocks.

Its application for the description of the behavior of the soil massifs has proved to be fruitful and has made it possible to analyze the failure of soils in practical problems of foundations, stability of slopes, tunnels, retaining walls, etc.

Several failure criteria have been established. Among them, the Mohr-Coulomb failure criterion (Figure 2) which is the most used in the practice of geotechnical engineering to describe in an approximate way the behavior of coarse-grained soils (*sand and gravel*) and the drained behavior of saturated fine soils (*silt and clay*) [5].

The Mohr-Coulomb failure criterion is schematized in the Mohr stress plane (Figure 2 (a)) by the equations:

$$\tau = \sigma' \tan \phi' + c \tag{1}$$

In terms of the principal effective stresses (σ'_1, σ'_3) (Figure 2 (b)), it is also written:

$$\sigma'_1 - \sigma'_3 = (\sigma'_1 + \sigma'_3) \sin \phi' - 2c' \cos \phi' \tag{2}$$

With:

- σ'_1, σ'_3 : major and minor effective stresses,
- ϕ' : internal friction angle,
- c : cohesion. The perfectly plastic linear elastic behavior with the Mohr-Coulomb failure criterion (Figure 2 (b)) is characterized by a linear elasticity (E, ν) and a plasticity threshold, defined by the cohesion c' , the internal friction angle ϕ' , in addition to the initial state.

At least two triaxial tests must be performed at different confining pressures to determine the parameters of the model. The yield surface $F(\sigma_{ij})$ is expressed as follows:

$$F(\sigma'_{ij}) = (\sigma'_1 - \sigma'_3) - (\sigma'_1 + \sigma'_3) \sin \phi' - 2c' \cos \phi' = 0. \tag{3}$$

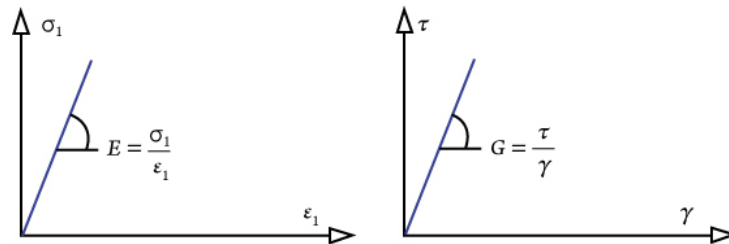


Figure 1. Linear elastic behavior law [1]

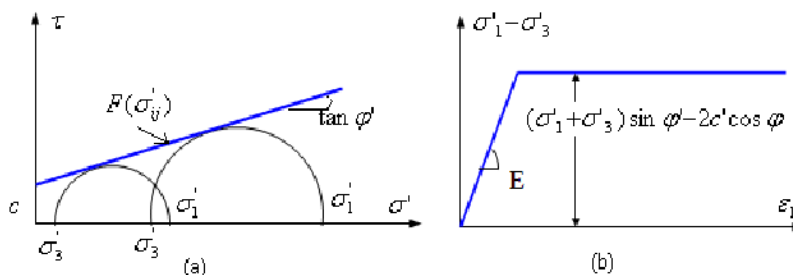


Figure 2. Behavior elastic law, perfectly plastic of Mohr-Coulomb [1]

2.2. Numerical Modeling of Foundations

A number of authors has proposed the basic principles of the finite elements method and its application for solving problems such as the study of the behavior of foundations over the last twenty years [10-17].

Several methods for modeling discontinuous behavior at the soil-structure interface have been proposed. These different methods led to the development of several digital tools dedicated to the study of foundations (*Ansys, Plaxis, Optum G2 ...*).

In this work, OptumG2 is used because it allows taking into account the various laws of soil behavior.

2.3. Optum Presentation

Optum G2 is a finite elements computation software featuring many analysis types including elastoplastic deformation analysis, seepage, and staged construction analysis. It provides full integration of limit, elastoplastic and seepage analysis, providing an ideal platform for both analysis and design. Optum G2 contains a range of finite elements including the popular 6-node and 15-node triangles. Its computational core builds on state-of-the-art algorithms that lead to an unprecedented efficiency and robustness – independent of the complexity of the constitutive model, number of elements in the mesh, etc. Optum allows to model works from several angles of analysis (internship) namely:

- limit analysis to determine the maximum stress at break and the associated deformations and displacements,
- force reduction analysis for the determination of safety factors;
- elastoplastic analysis for service analysis and staged construction;
- infiltration analysis for the partially saturated flow;
- Initial stress analysis for the determination of in-situ stress based on the soil pressure coefficient;
- Structural elements for modeling walls, anchors, geotextiles, etc.
- Adaptability of the mesh for all types of analysis.

In addition, a number of standard materials with parameters representing common geomaterials and structural elements are available.

3. Results and Discussion

3.1. Influence of the Young Modulus (*E*) on the Behavior of a Clay Mass

In this part, it is proposed to study the influence of the variation of the Young's modulus on the behavior of a clay mass. For this, a foundation of $2.5 \times 1 \times 0.7$ m resting on clay and subjected to a stress of 90 kN/m^2 is considered.

The soil is governed by a Mohr-Coulomb behavior law, which is used to describe coarse-grained soils (sand and gravel) and fine-grained soils (clays and silts) at long term. For the purposes of the study, the analysis is conducted on different angles:

- “Multiplier Elastoplastic” analysis may be seen as combining the Limit Analysis and Elastoplastic

analysis. As in Limit Analysis, the Multiplier loads are amplified until collapse while fixed loads and gravity are kept constant. This is done in a systematic elastoplastic manner with deformations computed at each load step.

- “Consolidation analysis” allows visualizing the degree of consolidation according to the duration of the application of the charges.

The input data of the study are given in Table 1 below:

Table 1. Input parameters of the study for different values of the Young's modulus $E= 20 \text{ MPa}$, $E= 25 \text{ MPa}$ and $E= 30 \text{ MPa}$,

Cohesion <i>C</i> (kPa)	10
Internal friction angle ϕ (°)	25
Dry density γ_d (kN/m ³)	20
Saturated density γ_{sat} (kN/m ³)	20
Poisson's ratio ν	0.25

The Figure 3 gives the modeling of the whole domain.

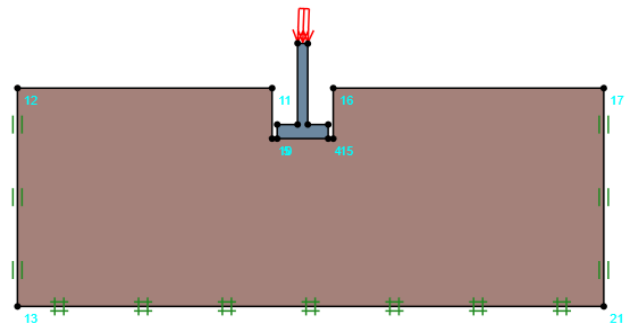


Figure 3. Rectangular foundation resting on clay

With a Young's modulus variation of 20 to 30 MPa, the clay behaves differently under static loading. This difference will be understood with the plotting of the deformation curves and the degree of consolidation. Thus, a good visualization of the initial and final displacements will also make it possible to understand the resistance aspect of the soil with different value of *E*, as shown in the following Figure 4.

The following Table 2 shows the evolution of the maximum values of the deformation, the maximum stress, the displacement and the load factor for various values of Young's modulus *E*.

Table 2. Results for different values of *E*

Young modulus <i>E</i> (MPa)	Maximum stresses σ (kPa)	Maximum Deformations ϵ (%)	Maximum Displacements <i>U</i> (m)	Laod multiplier
20	783,9	5,307	0,8126	35,13
25	942,8	4,453	0,688	36,04
30	776	3,47	0,525	35,43

The results show (Figure 5) also that each value of the Young's modulus is associated to a stress-strain curve and a consolidation curve.

For consolidation analysis over time, Figure 6 gives the results for the different values of *E*.

The analysis of the curves (stresses-deformations) of Figure 5 shows that the value of the modulus of elasticity has a more or less significant influence on the behavior of the foundation soil.

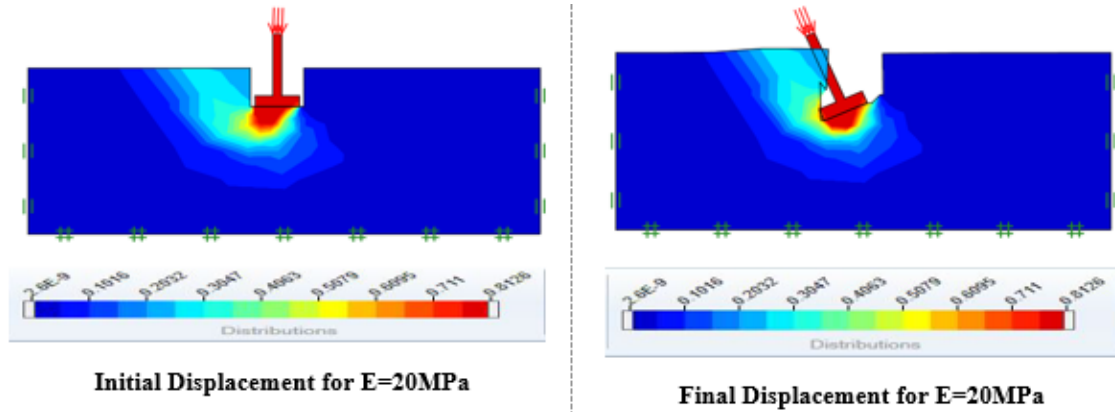


Figure 4. Mapping of displacements according to the variation of the modulus of elasticity

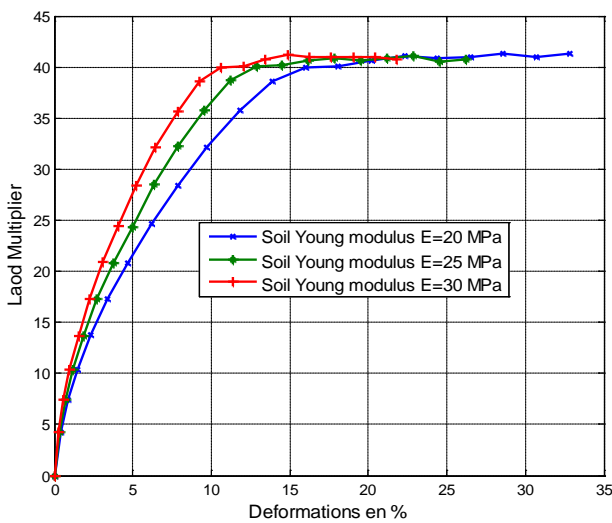


Figure 5. Deformations versus load for different values of the soil Young's modulus

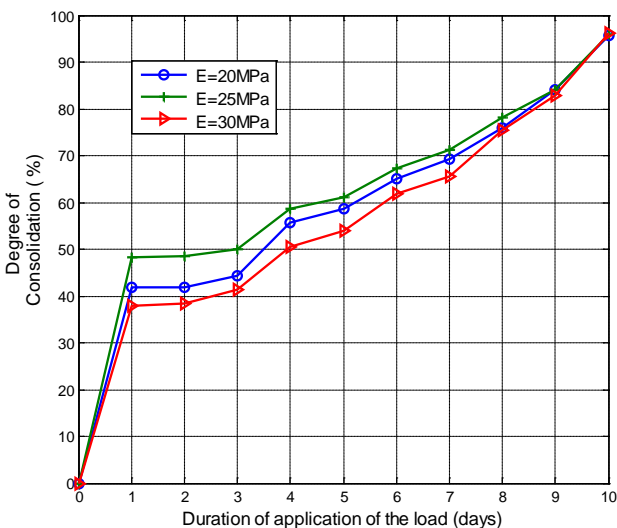


Figure 6. Evolution of the degree of consolidation U (%) according to the duration of the loading application

Indeed the study shows that with the variation of the modulus of elasticity (E), the clay becomes more and more stiff and ductile. For a Young's modulus of 30 MPa, the displacement in the clay mass reaches a maximum value of 0.525 m under a maximum stress of 776 kPa,

whereas for E rising from 25 to 20 MPa the maximum displacement goes from 0.688 to 0.813 m under constraints 942.8 and 783.9 kPa respectively.

The analysis shows, for a given stress value, a decrease of the deformations when the ductility of the clay increases (example for a load of $2700 \text{ kN} / \text{m}^2$ the clay with Young modulus $E = 30 \text{ MPa}$ records a deformation of 5.5 while that of 25 and 20 MPa reach values of 6.5 and 8.00).

The analysis of consolidation is essential in understanding the phenomena of settlement and is then the second angle of study. Thus, Figure 6 shows the evolution of the degree of consolidation as a function of the loading time, for different values of the Young's modulus.

It is noticed that on a loading day the curves give different values of degree of consolidation. Indeed 52% for $E = 20 \text{ MPa}$ and respectively 42 and 40 % for $E = 25 \text{ and } 30 \text{ MPa}$. However, at 10 days of loading, there is a convergence of the results for the different values of E (99 % as the degree of consolidation).

This is explained by the fact that more the Young's modulus is lower, more the material is compressible, so in the short term the clay with $E = 20 \text{ MPa}$ releases more vacuum or water (if it is saturated); therefore the deformations are more important. In the same way, more the clay with $E = 20 \text{ MPa}$ is consolidated (that is to say a decrease of the volume of the voids), more it evolves as those of $E = 25 \text{ and } 30 \text{ MPa}$. This shows that the modulus of elasticity of the soil mass depends on the state of consolidation.

3.2. Influence of the Poisson's Ratio ν on the Behavior of a Clay Mass

The coefficient is one of the important parameters for studying the behavior of foundation soils. Indeed, it allows determining the shear modulus of the ground G and its variation constitutes one of the angles of analysis of this work. The input parameters of the study are given in Table 3 below.

Table 3. Input data of the study for different values of Poisson's ratio ($\nu=0.2, \nu = 0.23$ and $\nu = 0.27$)

Cohesion C (kPa)	10
Internal friction angle ϕ ($^\circ$)	20
Dry density γ_{sec} (kN/m ³)	20
Saturated density γ_{sat} (kN/m ³)	20
Young's modulus E (MPa)	25

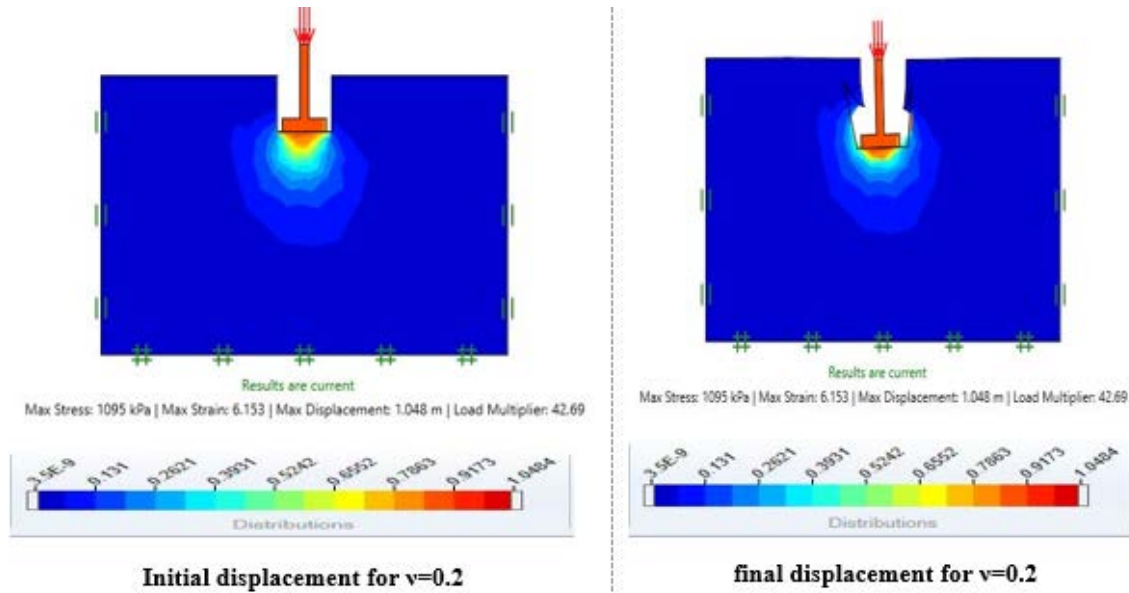


Figure 7. Mapping of displacements for various values of the Poisson's ratio

The same foundation that was used to study the influence of Young's modulus on soil behavior is repeated to study the effect of variation of Poisson's ratio. Displacement mapping is given in Figure 7.

The following Table 4 gives the evolution of the maximum values of the deformation, the maximum stress, the displacement and the load factor for various values of Poisson's ratio ν .

Table 4. Result for different value of Poisson's ratio

Poisson's ratio ν	Maximum stresses σ (kPa)	Maximum deformations ϵ (%)	Maximum Displacements U (m)	Laod Multiplier
0,2	1095	6,153	1,048	42,69
0,23	1054	7,546	1,037	42,79
0,27	1101	9,129	1,272	43,33

Figure 8 gives the stress-strain curves for various values of Poisson's ratio.

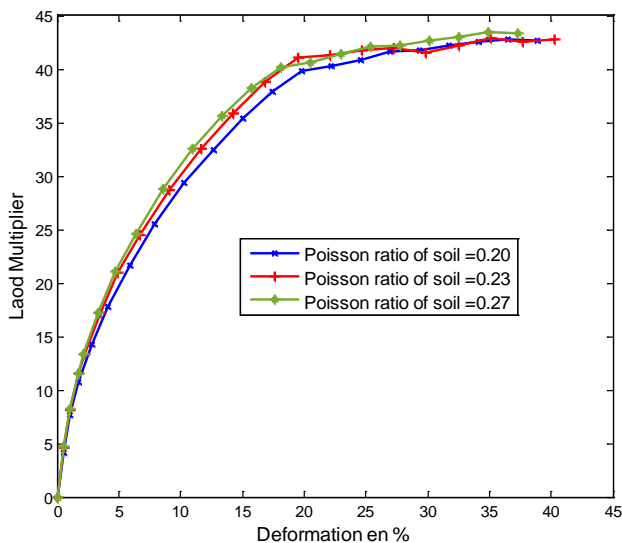


Figure 8. Deformation variation versus stresses for different values of the Poisson's ratio

The "Multiplier Elastoplastic" analysis shows an evolution of the rupture stress with respect to the variation of the Poisson's ratio. Indeed, with a value of the multiplicative factor of 30, there is a slight variation in the deformations; 11.2%, 9.8%, 8.8% (which corresponds to the respective displacement of 33cm, 29.4cm, and 26.4cm) for respective values of ν equal to: 0.2, 0.23, and 0.27. This small variation is explained by the fact that the Poisson's ratio does not influence the deformations, but affects the soil shear modulus G .

3.3. Influence of the Rupture Criterion on the Behavior of a Clay Mass

This part aims to study the clayey mass under various laws of behavior in order to discuss the strengths and limitations of different models of soil behavior. For the purposes of the study, the following models are adopted:

- The Mohr-Coulomb model, used for coarse-grained soils (sand and gravel) and for long-term cohesive soils (clays and silts).
- The Tresca model which is used for the study of saturated, undrained, fine-grained soils (clay, silt), in short-term total stresses, during which the variation of volume is zero.
- The AUS (Anisotropic Undrained Shear) model can be considered as another development of the generalized Tresca model. It is a total stress model describing clays and similar materials.

Input parameters include material data which can be determined by standard, undrained laboratory tests. The special characteristics of the AUS model include:

- Reinforcement of the load surface of the generalized Tresca model. This surface is uniform in materials with friable behavior, including clays, under undrained conditions and in general state of stress.
- Direct specification of undrained shear strengths in triaxial compression, triaxial expansion, and simple shear.
- Distinction between secant elastoplastic stiffness in compression and triaxial extension.

As a model of total stress, the AUS model does not require drainage data and no excess pore pressures are calculated. The input parameters of the problem are presented in Table 4, which follows.

Table 5. Input parameters

General characters		Specific characters	
Maerial model	Mohr-coulomb	General	
Reducible strength	yes	ID	4
Drainage		Unit weight type	Favourable
Drainage	Drained/undrained	Material	
Cavitation cut-off	No	Name	Firm-Clay MC
Stiffness		colour	Click to chose
E(MPa)	20	Material model	Tresca
ν	0.25	Reducible strength	Yes
Flow rule		Stiffness	
C (kPa)	10	Parameter Set	A
ϕ (°)	25	Eu (MPa) = 20MPa	with : $\epsilon_c,50$ (%) = 1 and $\epsilon_e,50$ (%)=3
Tension cut-off	no	Strength	
Fissures	No	Option	anisotropic
Unit weights		Su (kPa)	30
γ_{dry} (kN/m3)	18	Tension cut	No
γ_{sat} (kN/m3)	20	Linear Hydraulic model	
Hydraulic model	Linear	with $K_x = K_y = 10\text{-}5\text{m/day}$	
Condition initial K_o	0.50		

Figure 9 below gives the definition of the field of study.

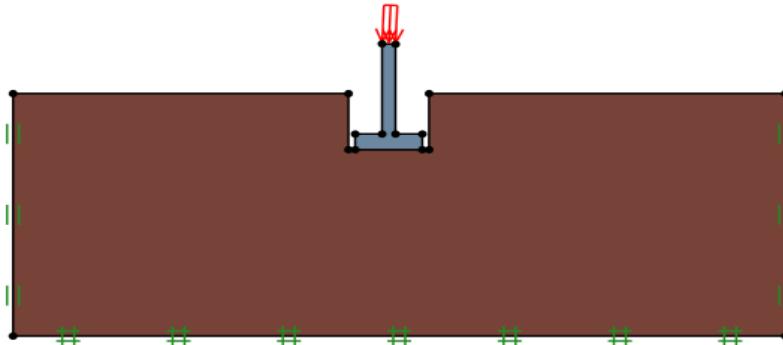


Figure 9. Foundation resting on clay

The results show that for each law of behavior, the foundation reacts differently. Figure 10 shows the displacement map for a Mohr-Coulomb model.

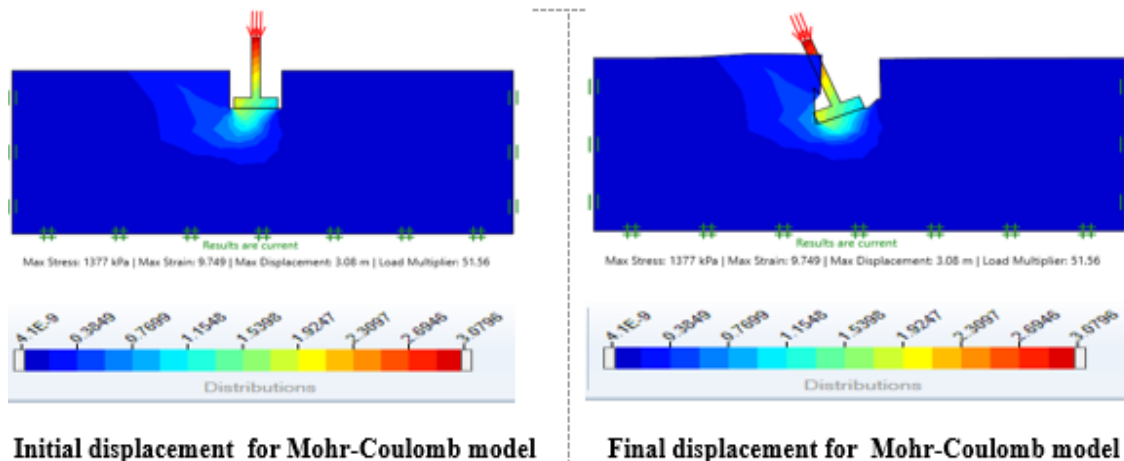


Figure 10. Cartographie des déplacements suivant la variation des critères de rupture

Table 6 below gives the evolution of the maximum values of the deformation, the maximum stress, the displacement and the load factor for various laws of behavior.

Table 6. Result of calculation for different soil models

Material behavior model	Maximum stresses σ (kPa)	Maximin déformation ϵ (%)	Maximum displacement U (mm)	Laod multiplier
Mohr-coulomb	1377	9,749	3,08	51,56
Tresca	247	2,323	0,4962	9,975
AUS	245,3	3,808	0,648	9,706

The results obtained (in stress-strain) for each constitutive law are shown in Figure 11:

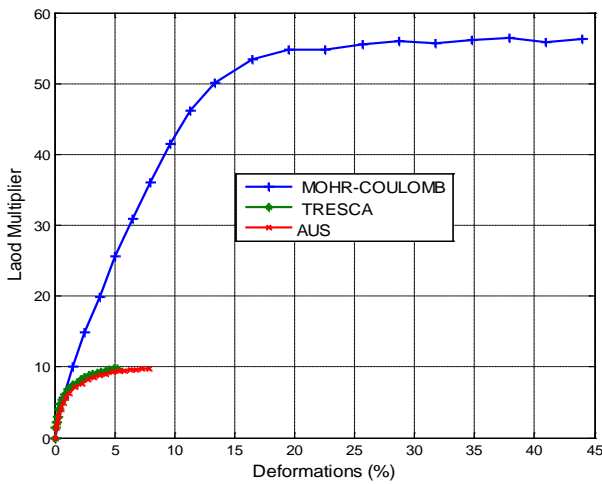


Figure 11. Stress-strain curves

These results show the variation of the deformations according to the loadings for different rupture criteria. The study of clay behavior by the Tresca and AUS models gives relatively low maximum deformations of 5.26 and 7.83% while the Mohr-Coulomb model leads to a deformation of 45.8%. The study shows that when the Mohr-Coulomb model is at 20% of its elastic reserve, the other models have already reached their rupture. This analysis shows that the Tresca and AUS models give similar results in the case of clay. In fact, the criteria of Tresca and AUS do not vary with the amplitude of the stresses, contrary to the Mohr-Coulomb criterion.

This means that the shear stress leading to rupture of the soil is much higher in the Mohr-Coulomb model than in models Tresca and AUS. This shows that model Mohr is more suitable for studying the behavior of clay.

3.4. Influence of the Variation of the Friction Angle of a Soil on its Mechanical Resistance

In this part, a continuous footing resting on two layers is modeled. The first layer is a sand and the second layer is a clay as shown in Figure 12 below:

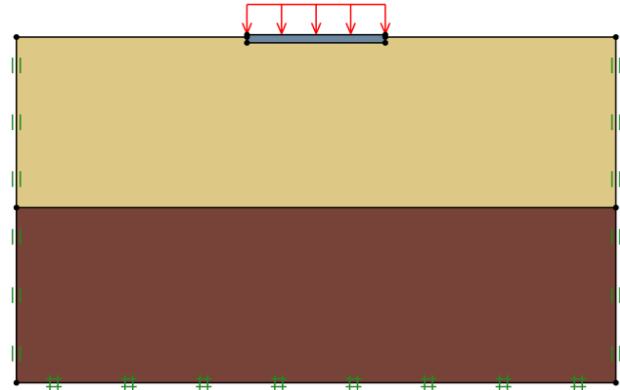


Figure 12. Schéma de la modélisation

The input data are recorded in Table 7:

Table 7. Characteristics of the two Foundation layers

Mecanical properties	1 st layer (Loose Land-MC)	2 nd layer (Firm Clay-MC)
	Mohr-Coulomb	Mohr-Coulomb
E (MPa)	20	25
ν	0.2	0.3
C (kPa)	0	10
ϕ (°)	40	20
γ_{dry} (kN/m ³)	14	20
γ_{sat} (kN/m ³)	19	20

A continuous footing of 12 m long is subjected to a surface load of $50 \text{ kN} / \text{m}^2$. The Figure 13 gives the initial and final displacements for $\phi = 30^\circ$.

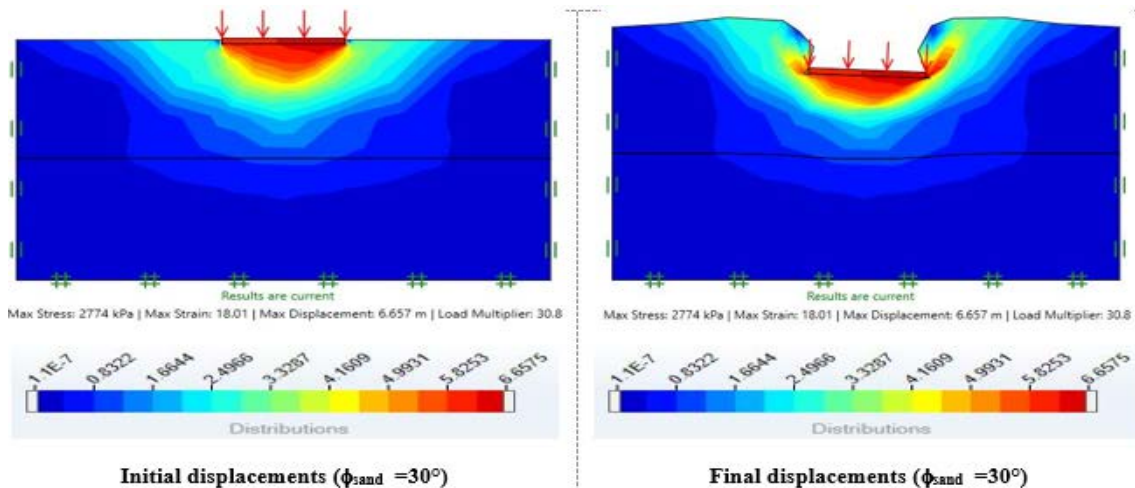


Figure 13. Mapping of initial and final displacements for a given angle of friction ϕ

Table 8. Results for various values of φ

Angle de frottement interne ($^{\circ}$)	Contraintes max σ (kPa)	Déformations max ε (%)	Déplacements max U (m)	Multiplicateur de chargement
30	2774	18.01	6.657	30.8
35	3408	22.46	8.155	44.93
40	4302	38.39	15.79	59.85

Table 8 shows the evolution of the maximum values of the deformation, the max stress, the displacement and the load factor for various for various values of the angle of friction. The results obtained are recorded in below Figure 14.

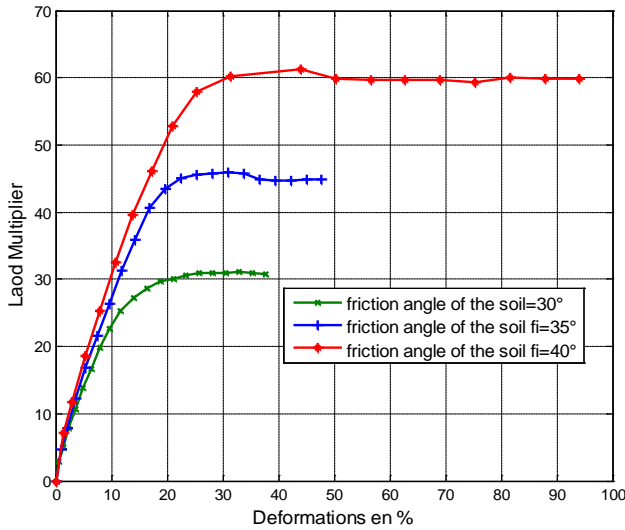


Figure 14. Loading versus deformations

It is found that when the internal friction angle of the sand is varied of 30° , 35° and 40° , an increase of the elastic limit loads as well as deformations of fractures. Indeed, the elastic limit loads are obtained respectively by a multiplication of the initial charge of 30, 43 and 60 with corresponding deformations of 17%, 20% and 25%. However, this can be explained by the fact that the relative density of the soil has a direct influence on the internal friction angle φ and, in other words, on its shear strength.

3.5. Influence of the Internal Cohesion of a Soil on the Mechanical Resistance

In this part, we always keep the hypotheses of the previous simulation except that instead of the friction angle of the sand, we vary the cohesion of the clay layer (10, 15 and 20 kPa) and we study its influence on the mechanical behavior of the soil mass. The results obtained by varying the cohesion of the clay layer (10, 15 and 20 kPa) are summarized in Figure 15.

The following Table 9 shows the evolution of the maximum values of the deformation, the max stress, the displacement and the load factor for various values of the cohesion C of the foundation soil.

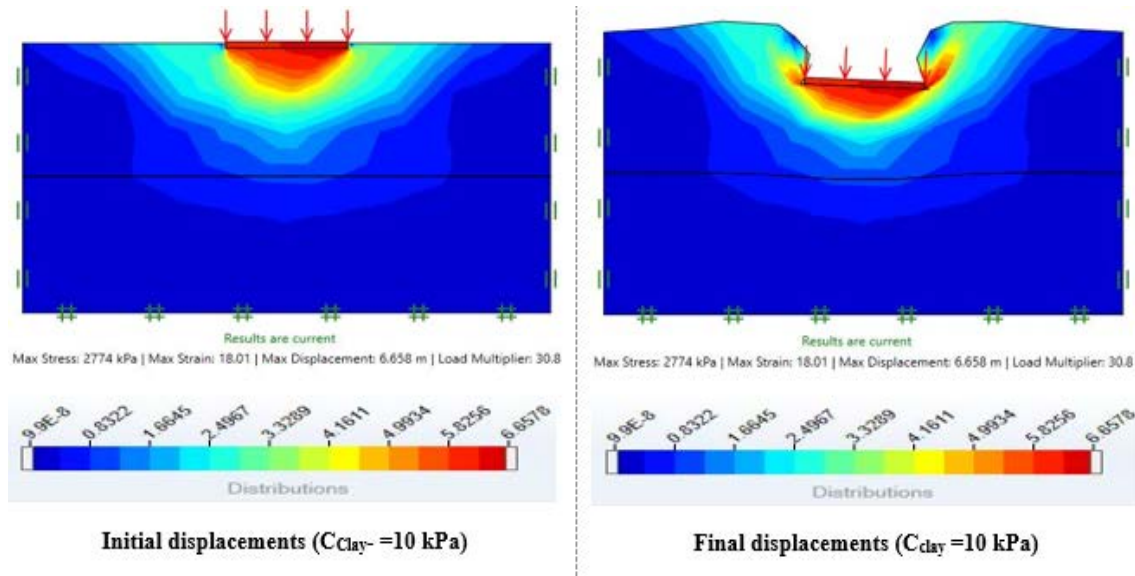


Figure 15. Mapping of displacements for different values of cohesion C

Table 9. Result for different values of C

Cohesion of clay	maximum stresses (kPa)	maximum deformation (%)	maximum displacement (m)	Laod Multiplier
$C=10kPa$	2774	18.01	6.66	30.08
$C=15kPa$	2659	17.47	6.80	30.55
$C=20kPa$	2665	17.96	6.76	30.29

The following Figure 16 give the corresponding deformation values at loading levels of a soil mass with a variation of the cohesion values of its second layer.

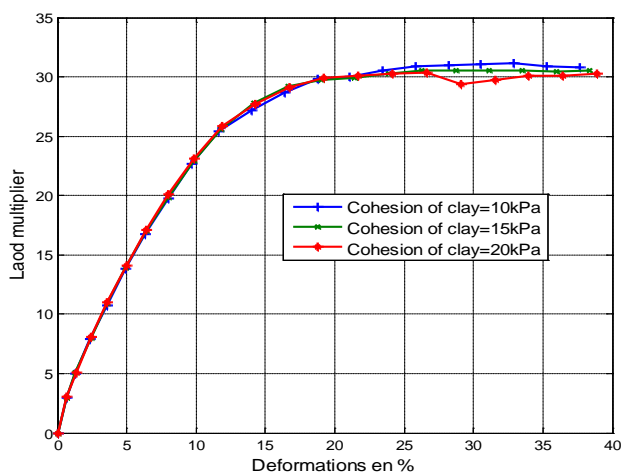


Figure 16. Load multiplier- deformations for various values of the cohesion of the second layer of soil

The study shows a very weak influence of the cohesion of the second layer of the soil mass (*clay*) on the mechanical behavior of the latter (as shown by the cartography of displacements ...). Indeed, this influence is apprehensible only in the plastic domain (*in the elastic domain the curves are combined*) (Figure 16).

Thus, the maximum displacement at rupture, for the three scenarios (cohesive soils $C = 10.15$ and 20 kPa), vary respectively from 6.66, 6.80 and 6.76 m under constraints of 2774, 2659 and 2665 kPa. This weak influence can be explained by the fact that the clay sand interface is a little distant from the base of the footing (*around 14.30 m*) and that displacements decrease considerably at this depth

4. Conclusion

The results obtained show that with the increasing variation of the modulus of elasticity (E), the clay becomes more and more stiff and ductile. For a given stress value, there is a decrease in deformations as the ductility of the clay increases. In the consolidation analysis, it can be seen that the lower the Young's modulus, the more compressible the material. This shows that the modulus of elasticity of the soil mass depends on its state of consolidation. The study shows that the variation of the Poisson's ratio has a weak influence on the deformations, but affects the shear modulus G of the soil.

The analysis shows, on the one hand, that the shear stress that leads to soil failure is much greater in the Mohr-Coulomb model than in the Tresca and AUS models and on the other hand that the Mohr-Coulomb model is more general and more suitable for studying the behavior of clay.

The study reveals that the law of behavior, the intrinsic properties (cohesion, modulus of elasticity, rupture criterion, angle of friction) and the lithology of the soil mass conditions the mode of ruin of the structure.

References

- [1] Sall O. A. (2015). "Calcul analytique et Modélisation de Structure en Plaque - Interaction Sol/Structure en vue du calcul des fondations superficielles en forme de radier", Thèse de doctorat a université de Thiès- 164 pages.
- [2] Sall O. A., Fall M., Berthaud Y., Ba M., Ndiaye M. "Influence of the Soil-Structure Interaction in the Behavior of Mat Foundation" *Open Journal of Civil Engineering*, 2014, 4, 71-83.
- [3] Sall O. A., Ba M, Ndiaye M, Sangare D, Fall M., Thiam A. (2015). Influence of Mechanical Properties of Concrete and Soil on Solicitations of Mat Foundation. *Open Journal of Civil Engineering*, 2015, 5, 249-260.
- [4] Sall O. A., Ba M., Sarr D., Ngom D. et Seye M. A. (2017). "Prise en compte de l'interaction sol-structure dans l'étude du comportement des pieux sous charge axiale" *Afrique SCIENCE 13(6) (2017) 435-445*, ISSN 1813-548X, <http://www.afriquescience.info>.
- [5] Nguyen P. P. T. (2008). Etude en place et au laboratoire du comportement en petites deformations des sols argileux, Thèse de doctorat de l'Ecole Nationale des Ponts et Chaussées, Paris 226 pages.
- [6] Hicher P. Y. (1985). Comportement des argiles saturées sur divers chemins de sollicitations monotones et cycliques. Application a une modélisation elastoplastique et viscoplastique. *Thèse de doctorat d'Etat*, Université Paris VI.
- [7] Bund H. (2009). "An Improved Method for Foundation Modulus in high way Engineering". *EJGE Vol. 14*, 2009.
- [8] Gerolymos N. (2009), "Numerical modeling of centrifuge cyclic lateral pile load experiments". *Earthquake Engineering and Engineering Vibration Vol.8, No.1 p 61-76*.
- [9] Hazzar L. (2014), "Analyse numérique de la réponse des pieux sous sollicitations laterals". Thèse de doctorat, université de Sherbrooke Canada. p214.
- [10] Haïtem (2017). "Etude de l'effet de l'interaction sol structure ISS sur la réponse dynamique des structures en béton armé", Thèse doctorat université de Batna 2 -259pages.
- [11] Grange (2008). "Modélisation simplifié en 3D de l'interaction sol-structure application au génie parasismique", Thèse pour l'obtention du grade de docteur de l'institut polytechnique de Grenoble – 173 pages.
- [12] Nancy (2016). "journées nationales de géotechnique et de géologie de l'ingénieur: Apports de l'interaction sol-structure dans la conception des fondations" -8 pages.
- [13] Nawel (2010). "Influence de l'interaction sol-structure dans la réponse sismique des bâtiments", Mémoire pour l'obtention du diplôme d'ingénieur – 140 pages.
- [14] Roussillon (2006). "Interaction sol-structure et interaction site-ville: aspects fondamentaux et modélisation", Thèse de doctorat à l'INSA de Lyon -309 pages.
- [15] Tchakou A. (2017). "Modélisation numérique du comportement d'un pieu dans un massif de fondation sous charge axiale avec Ansys", Projet de fin d'études d'ingénieur de conception, UFR SI, Université de Thiès, 79 pages.
- [16] Seghir, (2011). "Contribution à la modélisation numérique de la réponse sismique des ouvrages avec interaction sol-structure et interaction fluide-structure: application l'étude des barrages poids en béton", Thèse de doctorat a université de Bejaia -201 pages.
- [17] Zhang X. W., (2011). "Modélisation physique et numérique des interactions sol-structure sous sollicitations dynamiques transverses", Thèse de doctorat a université Grenoble -177 pages.

